Freeze Casting of Porous Hydroxyapatite Scaffolds. II. Sintering, Microstructure, and Mechanical Behavior

Qiang Fu,[1] Mohamed N. Rahaman,[1] Fatih Dogan,[1] B. Sonny Bal[2]

[1] Department of Materials Science and Engineering, University of Missouri-Rolla, Rolla, Missouri 65409

[2] Department of Orthopaedic Surgery, University of Missouri-Columbia, Columbia, Missouri 65212

Received 24 May 2007; revised 20 November 2007; accepted 18 December 2007
Published online 13 March 2008 in Wiley InterScience (www.interscience.wiley.com). DOI: 10.1002/jbm.b.31051

Abstract: In Part I, the influence of processing parameters on the general microstructure of freeze-cast hydroxyapatite (HA) constructs was explored. This work is an extension of Part I to investigate the effect of sintering conditions on the microstructure and mechanical behavior of freeze-cast HA. For constructs prepared from aqueous suspensions (5–20 vol % HA), sintering for 3 h at temperatures from 1250°C to 1375°C produced a decrease in porosity of <5% but an increase in strength of nearly 50%. Constructs with a porosity of 52% had compressive strengths of 12 ± 1 MPa and 5 ± 1 MPa in the directions parallel and perpendicular to the freezing direction, respectively. The mechanical response showed high strain tolerance (5–10% at the maximum stress), high strain to failure (>20%), and high strain rate sensitivity. Manipulation of the freeze-cast microstructure, achieved by additions of glycerol and 1,4-dioxane to the aqueous suspensions, produced changes in the magnitude of the mechanical response, but little change in the general nature of the response. The favorable mechanical behavior of the porous constructs, coupled with the ability to modify their microstructure, indicates the potential of the present freeze-casting route for the production of porous scaffolds for bone tissue engineering. © 2008 Wiley Periodicals, Inc. J Biomed Mater Res Part B: Appl Biomater 86B: 514–522, 2008

Keywords: biomaterials; scaffolds; hydroxyapatite; freeze casting; mechanical behavior

INTRODUCTION

In Part I, the influence of processing parameters on the general microstructure of porous hydroxyapatite (HA) constructs prepared by freeze casting of suspensions on a cold substrate was explored.[1] The effects of particle concentration of the suspension, temperature of the substrate, and modification of the solidification (freezing) behavior of the solvent by the addition of glycerol or 1,4-dioxane were investigated. Freeze casting of aqueous HA suspensions produced porous constructs with a uniform, lamellar-type microstructure in which plate-like HA lamellas were oriented in the direction of freezing. Changes in the particle concentration of the suspension and temperature of the cold substrate did not severely alter the lamellar-type microstructure but changed the porosity, the pore cross-section, and thickness of the HA lamellas. With increasing particle concentration in the suspension (5–20 vol %), the porosity and pore cross-section of the constructs decreased, but the thickness of the HA lamellas increased. The addition of 5–20 wt% of glycerol to the aqueous suspension resulted in sintered constructs with finer pores and a larger number of dendritic structures connecting the HA lamellas. On the other hand, the addition of 60 wt % of 1,4-dioxane to the aqueous suspension resulted in constructs with a cellular microstructure and larger pores. This work is an extension of Part I to investigate the effect of sintering conditions on the final microstructure and to characterize the mechanical behavior of the fabricated HA constructs.

In addition to being biocompatible, scaffold materials should have the ability to be formed into porous constructs with the relevant anatomical shape, as well as the ability to be formed economically and reproducibly. The fabricated scaffold should have the requisite microstructure to support tissue ingrowth. Interconnected or unidirectional pores with a mean diameter (or width) of 100 μm or greater, and open porosity of >50% are generally considered to be the minimum requirements to permit tissue ingrowth and function in porous scaffolds.[2,3] Scaffolds for load-bearing applications such as bone repair and regeneration should also possess adequate mechanical properties to support physiological loads.

Bone is generally classified into two types: cortical bone, also referred to as compact bone, and trabecular

Correspondence to: M.N. Rahaman (e-mail: rahaman@umr.edu)

TABLE I. Summary of Pore Characteristics and Compressive Strength of Porous Scaffolds Fabricated by a Variety of Methods

Technique	Material	Open Porosity (%)	Pore Size or Dimension (μm)	Compressive Strength (MPa)	Reference
Freeze casting	HA	47–52	5–30	12–18	Present work
	HA	50–65	80–110	7.5–20	
	HA	40–65	20	40–145	18, 19
TIPS	PLLA/HA (50:50)	90	50–200	0.4	20
	PLGA	93–94	50–60	0.38–0.58	21
	PDLLA/Biolgass®	93.5–94		0.07–0.08	22
	PLGA	90–96	114–137	0.2–0.9	23
	HA/Collagen	95	200–500	0.03	24
Polymer sponge	HA	86	420–560	0.21	25
	Glass reinforced HA	85–97.5	420–560	0.01–0.175	26
	HA	70–77	200–400	0.55–5	27
	45S5 Bioglass®	89–92	510–720	0.27–0.42	28
	$Ca_2MgSi_2O_7$	63–90	300–500	0.53–1.13	29
Gel casting	HA	76–80	20–1000	4.4–7.4	17
	HA	72–90	17–122	1.6–5.8	30
Solid freeform fabrication	PCL	61	360 × 430 × 620	3.1	15
	HA	35	334 × 469	30	16
	HA	41	250–350	34	17
Slip casting	13–93 glass	40–45	100–300	21–23	31
	HA	85	200–500	1.09–1.76	32
Gas foaming	PLGA	85–96	193–439	0.16–0.29	33
Fiber compacting	HA	13–33	50–500	6–13	34

bone, also referred to as cancellous or spongy bone. Cortical bone, found primarily in the shaft of long bones and as the outer shell around cancellous bone, is much denser, with a porosity of 5–10%.[4] Trabecular bone, found at the end of long bones, in vertebrae, and in flat bones such as the pelvis, is much more porous, with porosity in the range 50–90%.[5] The mechanical properties of bone vary between subjects, from one bone to another, and within different regions of the same bone. The mechanical properties are also highly anisotropic, as a result of the oriented microstructure. However, based on the testing of large specimens, the compressive strength and elastic modulus of cortical bone have been reported in the range 100–150 MPa and 10–20 GPa in the direction parallel to the axis of orientation (long axis).[6–8] The strength and modulus in the direction perpendicular to the long axis are typically 1.5 to 2 times lower. A wide range has been reported for the Young's modulus (0.1–5 GPa) and compressive strength (2–12 MPa) of cancellous bone.[7,8]

A variety of methods have been used to produce porous scaffolds for bone repair and regeneration, including consolidation with a pore-producing phase such as NaCl, starch, or PVA,[9–11] the use of foaming agents,[12–14] and solid freeform fabrication.[15–17] Table I provides a summary which is not meant to be exhaustive, but rather to indicate representative approaches. Freeze casting has been widely used for the production of synthetic polymer scaffolds, such as poly(lactic acid), PLA, poly(glycolic acid), PGA, and their coploymers, PLGA, as well as natural polymer scaffolds, such as collagen.[21,23,35] It has been applied more recently to the production of composites of HA and polymers (collagen or biodegradable polymers),[20,24] and to bioceramic (HA) scaffolds.[1,18,19] The low strength (typically <1 MPa) of porous constructs of synthetic and natural polymers, and HA-polymer composites is a limitation for the repair of load-bearing bones. Recent investigations have shown that porous HA scaffolds, with a lamellar-type microstructure and unidirectional pores, can be obtained by freeze casting of aqueous suspensions.[18,19] The microstructure and strength of the scaffolds can be modified by altering the particle concentration of the suspension, freezing rate, and sintering conditions. Compressive strengths as high as 65 MPa (56% porosity) and 147 MPa (47% porosity) in the direction parallel to the freezing direction were obtained by testing small thin disks (4 mm × 5 mm × 5 mm) cut from the freeze-cast sample. However, the pore width (or diameter) of these HA constructs (less than $\sim$20 μm) is too low for tissue ingrowth.

The objective of the present work was to investigate the effect of sintering conditions on the microstructure of the freeze-cast HA constructs and to characterize the mechanical behavior of the fabricated HA constructs. During sintering, it is expected that the HA lamellas, consisting of a packing of fine particles and fine pores, will undergo densification and grain growth, leading to an enhancement in strength. On the other hand, the unidirectional pores separating the HA plates are expected to undergo little change because the pore widths are much larger than the particle

(or grain) size of the HA plates.[36] Because the properties of the sintered constructs are controlled by their microstructure, an understanding of the microstructural development during sintering, as well as the influence of the microstructure on properties, is important.

MATERIALS AND METHODS

Cylindrical HA constructs (~8 mm diameter × 16 mm) were prepared by freeze casting suspensions (20 vol % particles) on a cold steel substrate (−20°C), and subliming the frozen liquid. The solvent in the suspensions consisted of water, a mixture of water and 5–20 wt % glycerol, or a mixture of water and 40–60 wt % 1,4-dioxane (referred to henceforth as dioxane). The glycerol and dioxane additions were used to modify the freezing (or solidification) of water, which provided an additional method for manipulating the microstructure of the freeze-cast constructs. The procedures were identical to those described in detail in Part I.[1]

Sintering was carried out in air for 3 h at temperatures between 1250°C and 1375°C, with a heating and cooling rate of 3°C/min. The microstructures of the cross-section of the green and sintered constructs were observed using scanning electron microscopy, SEM (S-4700, Hitachi Co., Tokyo, Japan). X-ray diffraction, XRD (D/mas 2550 v; Rigaku; The Woodlands, TX), was used to identify the phases present in the starting powder and sintered samples, using Cu K_α radiation ($\lambda = 0.15406$ nm) at a scanning rate of 1.8°/min in the 2θ range of 10–80°. The volume of open porosity in the sintered samples was measured using the Archimedes method. The grain size of sintered constructs was measured using the linear-intercept method.[24] More than 200 grain boundary intercepts were measured for the polished samples sintered at different temperature to obtain a mean value and standard deviation.

The mechanical behavior of the sintered constructs (~8 mm in diameter × 16 mm) in compressive loading was determined according to ASTM-C773 using an Instron testing machine (Model 4204, Norwood, MA) at a crosshead speed of 0.5 mm/min. Eight samples were tested, and the average strength and standard deviation were determined. The samples were tested in the directions parallel and perpendicular to the freezing direction. The crosshead speed of 0.5 mm/min is typical for the testing of dense specimens according to ASTM-C773. To investigate the strain-rate sensitivity of the compressive mechanical response, additional tests were performed at cross-head speeds of 0.05 mm/min and 5 mm/min. Cross-head speeds higher than 5 mm/min were impractical with the instrument and the size of specimens used.

The flexural strength of the sintered constructs was measured by loading unnotched cylindrical samples (~8 mm in diameter × 25 mm) at a crosshead speed of 0.5 mm/min in three-point bending (overall span = 20 mm) using an Instron testing machine (Model 4204). Eight specimens were tested. The flexural strength was determined from the equation

$$\sigma = \frac{8PL}{\pi d^3}$$

where P is the load applied to the specimens, L is the overall span, and d is the diameter of the specimens.

Strength and porosity values were determined as means ± standard deviations. Statistical analysis was carried our using one-way analysis of variance (ANOVA) and Turkey's post hoc test, with the level of significance set at $p < 0.05$.

RESULTS

Figure 1 shows the XRD patterns of the as-received HA powder, the powder calcined for 1 h at 900°C, and of the freeze-cast material sintered for 3 h at 1375°C, the highest sintering temperature used in the experiments. Each pattern corresponded to the reference pattern of HA (JCPSD 72-1243). The XRD peaks for the as-received powder were broader and had a lower intensity (peak height) than those for the sintered material, which is an indication that the as-received powder may have a size in the nanocrystalline range, incompletely crystallized, or a combination of both. Within the limits of detection by the XRD (<0.5 wt %), no additional peaks corresponding to any second phases could be found in the patterns. It has been reported that HA decomposed into tricalcium phosphate and tetracalcium phosphate at temperatures above ~1300°C,[37] and that this decomposition resulted in a sharp drop in strength and affected the osteocalstic resorption activity of HA.[38,39] However, for the HA powder used in the present work, the results indicated that sintering temperatures as high as 1375°C can be used without detectable decomposition. *In vitro* cell culture experiments are currently being performed to evaluate the effect of the sintered HA constructs

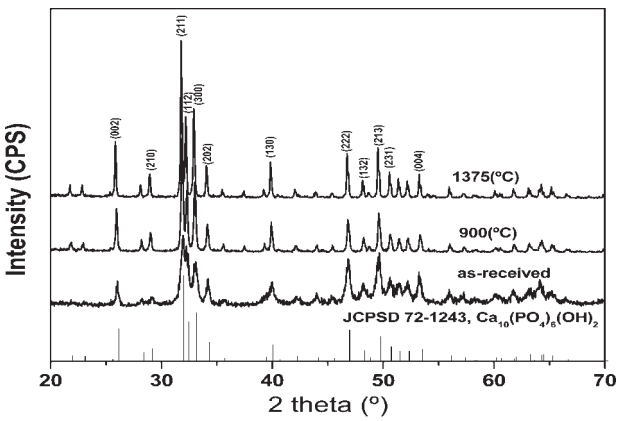

Figure 1. X-ray diffraction (XRD) patterns of the as-received HA powder, the powder heated for 1 h at 900°C, and the freeze-cast construct sintered for 3 h at 1375°C.

on cell viability and the ability of the constructs to support cell infiltration into the unidirectional pores.

The effect of the sintering temperature on the open porosity and compressive strength of HA constructs sintered for 3 h at temperatures between 1250°C and 1375°C is shown in Figure 2. The constructs were prepared from aqueous suspensions containing 20 vol % HA. With increasing temperature, the porosity decreased slightly, from a value of 55% at 1250°C to a limiting value of ~52% at 1350°C. This is an indication that the HA plates in the lamellar-type microstructure had reached their highest density at 1350°C. Sintering for much longer time at 1350°C or at higher temperatures will lead primarily to grain growth in the HA lamellas, without any increase in density. Therefore, sintering for 3 h at 1350°C can be taken as approximately the optimum sintering conditions for the present system. The compressive strength in the direction of freezing increased with sintering temperature (Figure 2), reaching its highest value of 12 ± 1 MPa at 1350°C, and showed no further improvement as the sintering temperature was increased to 1375°C. This increase in the compressive strength is a reflection of the decrease in porosity indicating that the strength improvement is controlled by the increase in density of the HA lamellas.

As observed in Part I,[1] the addition of glycerol to the aqueous solvent produced a modification of the freeze-cast microstructure, giving smaller pore diameters and resulting in a larger number of dendrites connecting the HA plates. Figure 3 shows the effect of glycerol additions on the porosity and compressive strength of the constructs sintered for 3 h at 1350°C. The constructs were prepared from suspensions with 20 vol % solids. The porosity decreased by ~6%, from ~52% to ~46%, as the glycerol concentration in the solvent increased from 0 to 20 wt %. On the other hand, the compressive strength (in the direction of freezing)

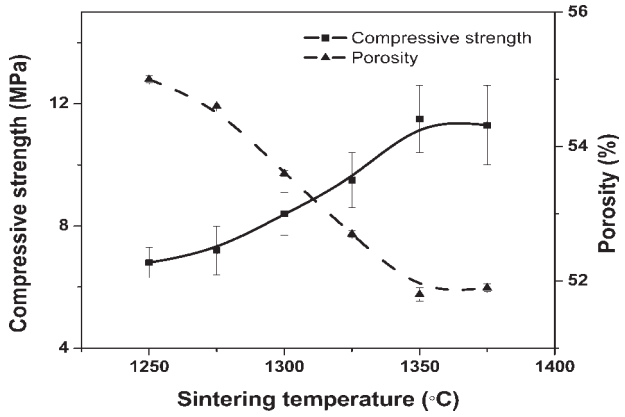

Figure 2. Influence of sintering temperature on the porosity and compressive strength (in the direction of freezing) of HA constructs prepared from aqueous suspensions with 20 vol % particles. All pairs of porosity were significantly different except the pair between 1350 and 1375°C (p = 0.99); all pairs of compressive strength were significantly different except the pairs between 1250 and 1275°C, 1300 and 1325°C, 1350 and 1375°C (p = 0.97, 0.22, 1.0, respectively).

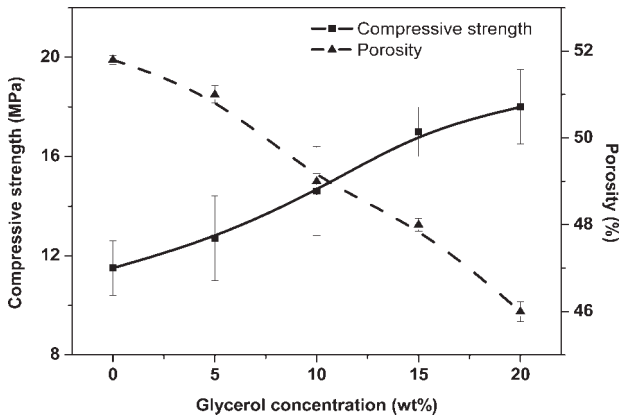

Figure 3. Effect of glycerol addition to the aqueous suspension (20 vol % particles) on the porosity and compressive strength (in the direction of freezing) of constructs sintered for 3 h at 1350°C. All pairs of porosity were significantly different; all pairs of compressive strength were significantly different except the pairs between 0 and 5, 5 and 10, 15 and 20 wt % glycerol (p = 0.69, 0.28, 0.50, respectively).

increased by ~50%, from 12 ± 1 MPa to 18 ± 2 MPa. This increase in the strength can be attributed to the finer pores, the lower porosity, the larger number of dendrites connecting the HA lamellas or a combination of the three.

Figure 4 shows stress–strain curves in compression testing for freeze-cast HA constructs prepared from aqueous suspensions (20 vol % HA) without glycerol and sintered for 3 h at 1350°C. The curves show the behavior of the constructs in the direction parallel and perpendicular to the freezing direction. The data shown are engineering stresses and strains, based on the initial cross-sectional area and length of the test sample, and do not represent the true stresses and strains. An interesting feature of the stress–strain response is the high strain tolerance of the constructs. Unlike common ceramics which show brittle behavior with

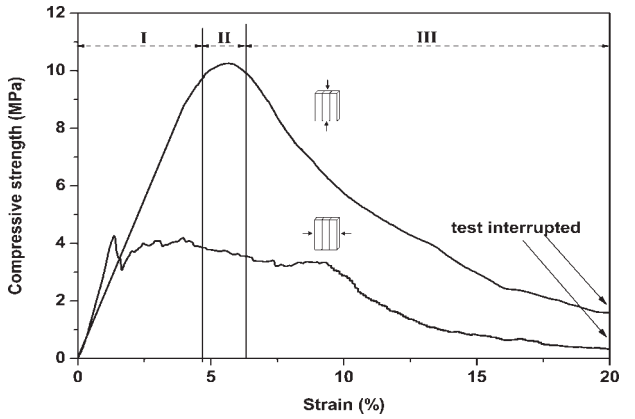

Figure 4. Stress–strain behavior in compression testing parallel and perpendicular to the freezing direction, for HA constructs prepared from aqueous suspensions (20 vol % particles) and sintered for 3 h at 1350°C. Three different regions are outlined for the curve corresponding to the parallel testing direction: I, elastic region; II, stress plateau region; III, failure region.

just an elastic response and failure at low strain (typically <0.1%), the constructs produced in the present work showed three distinct regions: an elastic regime in which the stress-strain response was linear, a stress plateau region representing a region of highest sustainable loading, and a failure region of decreasing load-beating ability. The elastic modulus, determined from the slope of the linear region, was 0.2 GPa. While the three regions can be observed in both curves, the stress–strain curve in the freezing direction had a different shape from that perpendicular to the freezing direction. In the freezing direction, the curve had a more smoothly varying, asymmetric bell shape, with a compressive strength (taken as the stress at the peak) of ~10 MPa at a strain of ~7%. In contrast, the curve for the perpendicular testing direction had a large plateau region, in a strain range of 2–10%, with numerous bumps and valleys. The average compressive strength in this plateau region was ~4 MPa. The small peaks and valleys in the curve presumably resulted from progressive breakage of the HA lamellas and the dendrites between the lamellas.

Figure 5 shows the effect of strain rate on the compressive mechanical response (in the direction of freezing) for constructs prepared from aqueous suspension (20 vol % HA). The response was quite sensitive to the rate of loading (taken as proportional to the cross-head speed). With increasing strain rate, the peak compressive stress increased in magnitude and shifted to lower strain. For the same specimen length (16 mm), increasing the cross-head speed from 0.05 mm/min to 0.5 mm/min and 5mm/min, produced an increase in the peak compressive stress of ~25 and ~125%, respectively. On the other hand, the strain at the peak compressive stress decreased from 8% to 5% and 2%, respectively.

Figure 6 shows the stress–strain curve in three-point bending for freeze-cast HA constructs prepared from aqueous suspensions (20 vol % HA) without glycerol and sintered for 3 h at 1350°C. The constructs showed a high strain tolerance (~6%) in flexure, similar in nature to the response observed in compression testing, indicating that the high strain tolerance is not just restricted to compression. The small peaks and valleys in the stress–strain curve presumably resulted from crack deflection during delamination of the HA lamellas. The flexural strength (taken as the stress at the peak of the stress–strain curve) was 2.5 ± 0.9 MPa at a strain of ~6%.

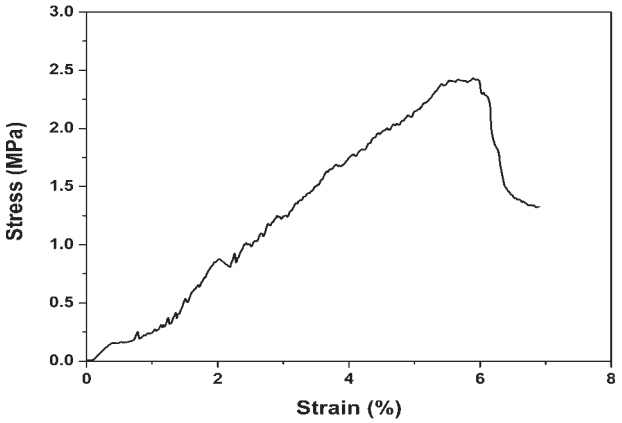

Figure 6. Stress–strain behavior in three-point bending for HA constructs prepared from aqueous suspensions (20 vol % particles) and sintered for 3 h at 1350°C.

The stress–strain behavior in compression for constructs prepared from suspensions (20 vol % HA particles) with 20 wt % glycerol and sintered for 3 h at 1350°C is shown in Figure 7. In general, the curves showed features similar to those for constructs prepared without glycerol, but the load-bearing capacity was higher. The compressive strengths in the directions parallel and perpendicular to the freezing direction were 18 ± 2 MPa and 7 ± 1 MPa, respectively, compared with values of 12 ± 1 MPa and 5 ± 1 MPa for similar constructs prepared from suspensions without glycerol. The elastic modulus in the direction of freezing, determined from the linear region of the curve, was 0.6 GPa. The use of glycerol also improved the strain tolerance, with the constructs able to support a stress of ~6 MPa at a strain as high as 20%.

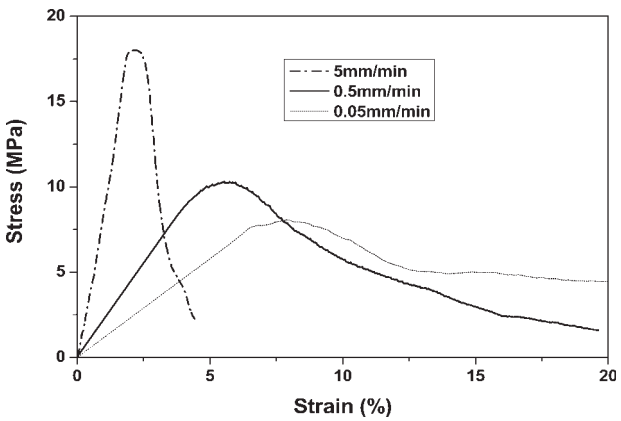

Figure 5. Effect of loading rate on the compressive mechanical response of HA constructs prepared from aqueous suspension with 20 vol % particles.

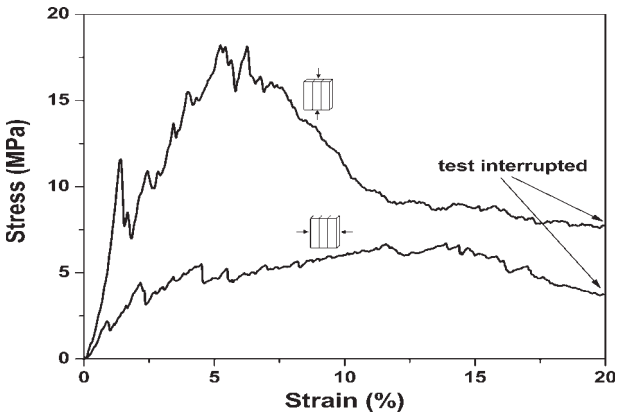

Figure 7. Stress–strain behavior of HA constructs prepared from suspensions with 20 wt % glycerol and sintered for 3 h at 1350°C. The load was applied in compression, parallel and perpendicular to the freezing direction.

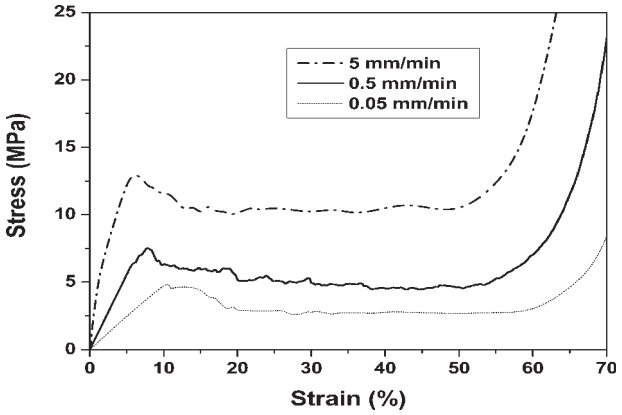

Figure 8. Effect of loading rate on the mechanical response of the HA constructs prepared from suspensions (10 vol % particles) containing 60 wt % dioxane.

Figure 8 shows the stress–strain curves, in the direction of freezing, for constructs prepared from suspensions (10 vol % HA particles) in which the solvent was 40 wt % water and 60 wt % dioxane. The mechanical response of these constructs showed a higher strain tolerance (~60%) than constructs prepared from aqueous suspensions (Figure 4) or from suspensions with glycerol (Figure 6). As observed for the testing of constructs prepared from aqueous suspensions (Figure 5), the mechanical response is also sensitive to the rate of loading. The stress–strain curve consisted of three distinct regions: an approximately linear regime, a plateau region in which the stress was almost constant with increasing strain, and a region of sharply rising stress. For testing at a cross-head speed of 0.5 mm/min, the peak compressive stress was 7.5 MPa at a strain of 8%. The elastic modulus, determined from the approximately linear region, was 0.1 GPa.

SEM images of the top and middle portions of an HA construct after completion of the compressive strength testing are shown in Figure 9. The construct was prepared from aqueous suspensions (without glycerol or dioxane) containing 20 vol % HA. A highly tortuous surface was observed at the top surface [Figure 9(a)], unlike the relatively smooth fracture surface commonly observed for brittle materials. The middle portion of the broken construct [Figure 9(b)], showed almost equally spaced cracks, perpendicular to the length of the HA lamellas. Furthermore, the cracks did not propagate across the entire sample. Instead, they appeared to terminate after traversing each HA lamella.

The fractured surfaces, following compressive strength testing, for the sintered constructs prepared from suspensions (20 vol % HA) with 20 wt % glycerol are shown in Figure 10. The top part of the fractured surface [Figure 10(a)] appeared to show tortuous crack patterns, not unlike those in Figure 9(a). Dendrites between the HA plates were also observed. When compared with the HA constructs prepared from suspensions without glycerol [Figure 9(b)], no cracks perpendicular to the length of the HA lamellas were observed [Figure 10(b)].This is presumably due to the fine pores and the presence of a larger number of dendrites between the HA lamellas, which provided an alternative fracture mechanism.

DISCUSSION

The present freeze casting route relied on densifying the HA lamellas, with little modification of the macropores between the lamellas, for developing the optimum strength of the construct. The results indicated that the optimum strength was achieved without any detectable change in the XRD pattern of the material by sintering for 3 h at 1350°C. For constructs prepared from aqueous suspensions (20 vol % HA) without glycerol or dioxane, the compressive strength in the direction of freezing (12 ± 1 MPa) was at the upper limit of the values for cancellous bone (2–12 MPa),[8] whereas the elastic modulus (0.2 GPa) was closer to the lower limit for cancellous bone (0.1–5 GPa).[8] The porosity (55%) was at the lower end for cancellous bone (50–90%), but the pore size (15 ± 10 μm) was considered to be too low to support tissue ingrowth.[40,41]

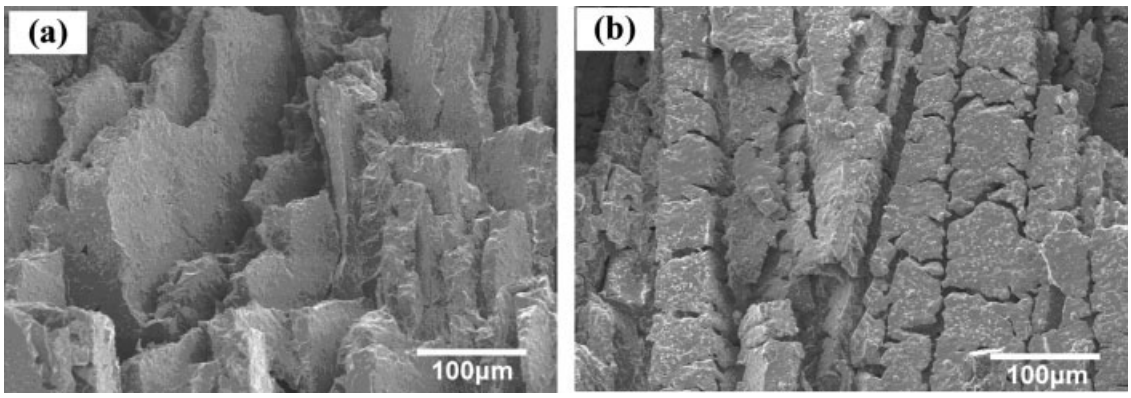

Figure 9. Fractured surfaces, after compression testing, of HA constructs prepared from suspensions without glycerol: (a) top surface, perpendicular to the freezing direction; (b) surface parallel to the freezing direction.

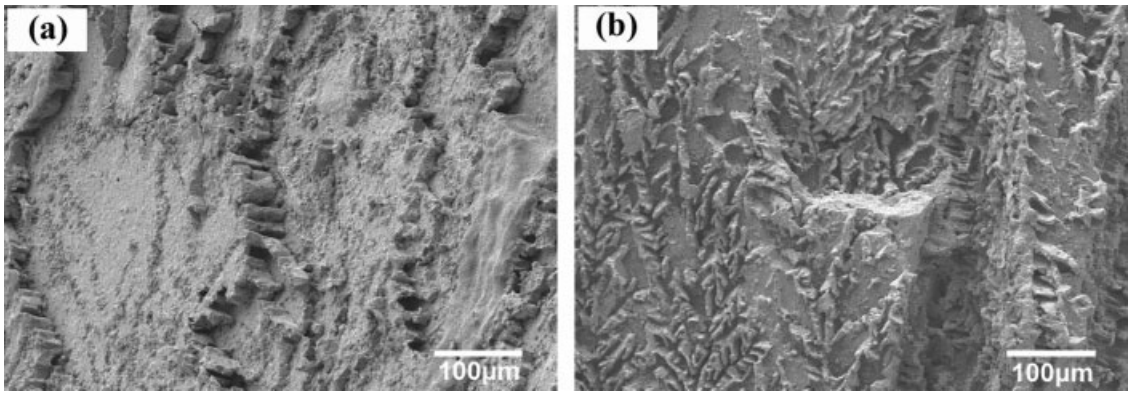

Figure 10. Fractured surfaces, after compression testing, of HA constructs prepared from suspensions with 20 wt % glycerol: (a) top surface, perpendicular to the freezing direction; (b) surface parallel to the freezing direction.

Because of differences in pore characteristics (such as porosity and pore size), a true comparison cannot be made between the strength values obtained in the present work and those summarized in Table I for constructs fabricated by a variety of methods. Nevertheless, the compressive strengths of the HA scaffolds fabricated in the present work were at least one order of magnitude higher than the values for polymer scaffolds or polymer–ceramic composites prepared by a unidirectional freeze casting method.[20–24] The strengths obtained in the present work were also one order of magnitude higher than those for porous bioceramic constructs with a more isotropic microstructure, such as those fabricated by infiltration of a polymer sponge or by a gas foaming technique.[12,25-27,28-30] Furthermore, the strengths were comparable with the values for porous bioceramic constructs fabricated by solid freeform fabrication routes and by more conventional methods.[15-17,31-34]

When compared with the results of Deville et al.,[18,19] who reported compressive strengths of 65 MPa (56% porosity) and 147 MPa (47% porosity) for HA constructs in the direction of freezing, the strengths obtained in this work were far lower. One factor which might contribute to the difference is the cooling rate of the suspension. The results of Deville et al.[18] showed a large increase in strength with increasing cooling rate, and the high strengths reported were for the highest cooling rate used. Faster cooling rates lead to the production of constructs with finer pores. While the strength was higher, the finer pores were less favorable for supporting tissue ingrowth. In the present work, the suspensions were frozen on a substrate at a fixed temperature (-20°C), and the cooling rate corresponded approximately to the lowest cooling rates used by Deville et al.[18] The compressive strengths obtained in the present work are comparable to the values reported by Deville et al. for the lowest cooling rates used in their work. There was also a difference between the sizes of the specimens used in the two studies. Deville et al.[18] used test samples (4 mm $\times$ 5 mm $\times$ 5 mm) cut from the sintered material in which the height to the cross-sectional width was only 0.8. In the present work, the as-fabricated specimens were tested according to ASTM-C773 in which the height to diameter ratio was >2.

An interesting property of the HA constructs prepared in this work was the high strain tolerance, leading to a high strain to failure (Figure 4). SEM images of the constructs after compressive strength testing [Figure 9(a)] showed a highly tortuous crack path. This type of tortuous fracture surface provided a large increase in the crack path, and has been proposed as an effective toughening mechanism in biological composites.[42] Furthermore, deflection, branching, and blunting of the cracks were also observed in the constructs after testing [Figure 9(b)]. These toughening mechanisms, coupled with the fine, homogeneous microstructure presumably resulted in delocalized failure, which provided the high strain tolerance observed in the stress–strain curves.

Similar to the behavior of bone[43,44] and other natural materials, the mechanical response of the HA constructs fabricated in this work was quite sensitive to the rate of loading (Figure 5). The elastic modulus and the compressive strength were observed to increase with higher loading rate but the strain to failure decreased. Since HA itself is brittle, the strain rate sensitivity resulted from the lamellar-type microstructure developed by the freeze-casting route.

The use of glycerol to modify the freezing behavior of the solvent resulted in the production of HA constructs with higher compressive strength and higher strain tolerance (Figure 7). The enhanced mechanical response presumably resulted from the lower porosity, smaller pores, and the larger number of dendrites between the HA lamellas.[1] More numerous peaks and valleys were also observed in the stress–strain curves (Figure 7), particularly in testing parallel the freezing direction, which presumably resulted from the progressive rupture of the larger number of dendrites between the HA lamellas. The additional work required to rupture these dendrites presumably provided a strong contribution to the increase in compressive strength and strain tolerance.[45]

As described in Part I,[1] addition of dioxane (60 wt %) to the aqueous suspension resulted in the production of HA constructs with a cellular microstructure and larger pores. Constructs prepared from suspensions with 10 vol % HA had a porosity of 65% and an average pore diameter of (100 ± 10 μm). These pore characteristics are considered to be more favorable for tissue ingrowth[2,3] when compared with the fine pores obtained in constructs prepared from aqueous suspensions with or without glycerol additions. The mechanical response of the HA constructs (Figure 8) was similar in nature to the response of bone and other natural materials such as wood and cork,[46] as well as the response of synthetic scaffolds with an oriented microstructure prepared by solid freeform fabrication techniques.[31] Furthermore, for a cross-head speed of 0.5 mm/min, the compressive strength (7.5 MPa), taken as the value at the peak stress, and the strain (8%) at the peak compressive stress were in the upper range of values for human cancellous bone (compressive strength = 2–12 MPa and strain to failure = 5–7%).[8] Based on their microstructure and mechanical response, these porous HA constructs prepared from aqueous suspensions with 60 wt % dioxane may provide favorable substrates for tissue engineering of bone. Experiments are currently being performed to evaluate the biocompatibility of the constructs and to optimize their mechanical response.

CONCLUSIONS

The compressive strength of freeze-cast HA constructs was strongly dependent on the sintering temperature used to densify the HA. Optimum strength was obtained after sintering for 3 h at 1350°C, presumably because of the HA lamellas in the porous structure reaching nearly full density. XRD indicated that no new phase was formed in the HA constructs after sintering at 1350°C. Constructs prepared from aqueous suspensions had compressive strengths of 12 ± 1 MPa and 5 ± 1 MPa in the directions parallel and perpendicular to the freezing direction, respectively, a flexural strength of 2.5 ± 0.9 MPa, and strain to failure of >20%. However, the porosity (52%) and pore size (5–30 μm) were considered to be too low to support tissue ingrowth. Constructs prepared from aqueous suspensions with 20 wt % glycerol had higher strength, but lower porosity and finer pores. HA constructs prepared from aqueous suspensions (10 wt % particles) with 60 wt % dioxane had a compressive strength of 7.5 MPa, strain to failure of 60%, and favorable microstructure for tissue ingrowth (porosity ~65% and pore size = 100 ± 10 μm). The mechanical response of the HA constructs was similar in nature to that for bone and other natural materials (high strain to failure and strain rate sensitivity). The favorable mechanical response of the porous constructs coupled with the ability to modify the microstructure and mechanical properties indicates the potential of the present freeze casting route for the fabrication of porous scaffolds for bone tissue engineering.

REFERENCES

1. Fu Q, Rahaman MN, Dogan F, Bal BS. Freeze casting of porous hydroxyapatite scaffolds. I. Processing and general microstructure. J Biomed Mater Res B: Appl Biomater. Forthcoming.
2. Hollinger JO, Leong K. Poly(α-hydroxy acids): Carriers for bone morphogenetic proteins. Biomaterials 1996;17:187–194.
3. Hu YH, Grainger DW, Winn SR, Hollinger JO. Fabrication of poly(α-hydroxy acid) foam scaffolds using multiple solvent systems. J Biomed Mater Res 2002;59:563–572.
4. Martin RB, Burr DB, Sharkey NA. Skeletal Tissue Mechanics. New York: Springer-Verlag; 1998.
5. Goldstein SA. The mechanical properties of trabecular bone: Dependence on anatomic location and function. J Biomech 1987;20:1055–1062.
6. Reilly DT, Burstein AH, Frankel VH. The elastic modulus of bone. J Biomech 1974;7:271–275.
7. Rho JY, Hobatho MC, Ashman RB. Relations of density and CT numbers to mechanical properties for human cortical and cancellous bone. Med Eng Phys 1995;17:347–355.
8. Fung YC. Biomechanics: Mechanical Properties of Living Tissues. New York: Springer; 1993. p 500.
9. Mikos AG, Sarakinos G, Leite SM, Vacanti JP, Langer R. Laminated three-dimensional biodegradable foams for use in tissue engineering. Biomaterials 1993;14:323–330.
10. Rodríguez-Lorenzo LM, Vallet-Regí M, Ferreira JMF. Fabrication of porous hydroxyapatite bodies by a new direct consolidation method: starch consolidation. J Biomed Mater Res 2002;60:232–240.
11. Li SH, De Wijn JR, Layrolle P, De Groot K. Synthesis of macroporous hydroxyapatite scaffolds for bone tissue engineering. J Biomed Mater Res 2002;61:109–120.
12. Sepulveda P, Binner JG, Rogero SO, Higa OZ, Bressiani JC. Production of porous hydroxyapatite by the gel-casting of foams and cytotoxic evaluation. J Biomed Mater Res 2000;50:27–34.
13. Almirall A, Larrecq G, Delgado JA, Martinez S, Planell JA, Ginebra MP. Fabrication of low temperature macroporous hydroxyapatite scaffolds by foaming and hydrolysis of an α-TCP paste. Biomaterials 2004;25:3671–3680.
14. Ebaretonbofa E, Evans JRG. High porosity hydroxyapatite foam scaffolds for bone substitute. J Porous Mater 2004;9: 257–263.
15. Hutmacher DW, Schantz T, Zein I, Ng KW, Teoh SH, Tan KC. Mechanical properties and cell cultural response of polycaprolactone scaffolds designed and fabricated via fused deposition modeling. J Biomed Mater Res 2001;55:203–216.
16. Chu T-MG, Oron DG, Hollister SJ, Feinberg SE, Halloran JW. Mechanical and in vivo performance of hydroxyapatite implants with controlled architectures. Biomaterials 2002;23: 1283–1293.
17. Woodard JR, Hilldore AJ, Lan SK, Park CJ, Morgan AW, Eurell JAC, Clark SG, Wheeler MB, Jamison RD, Johnson AJ. The mechanical properties and osteoconductivity of hydroxyapatite bone scaffolds with multi-scale porosity. Biomaterials 2007;28:45–54.
18. Deville S, Saiz E, Tomsia A. Freeze casting of hydroxyapatite scaffolds for bone tissue engineering. Biomaterials 2006;27: 5480–5489.
19. Deville S, Saiz E, Nalla RK, Tomsia A. Freezing as a path to build complex composites. Science 2006;311:515–518.

20. Zhang R, Ma PX. Poly(α-hydroxyl acids)/hydroxyapatite porous composites for bone-tissue engineering. I. Preparation and morphology. J Biomed Mater Res 1999;44:446–455.
21. Ma PX, Zhang R. Microtubular architecture of biodegradable polymer scaffolds. J Biomed Mater Res 2001;56:469–477.
22. Blaker JJ, Maquet V, Jérôme R, Boccaccini AR, Nazhat SN. Mechanical properties of highly porous PDLLA/Biolgass® composite foams as scaffolds for bone tissue engineering. Acta Biomater 2005;1:643–652.
23. Yang F, Qu X, Cui W, Bei J, Yu F, Lu S, Wang S. Manufacturing and morphology structure of polylactide-type microtubular orientation-structure scaffolds. Biomaterials 2006;27: 4923–4933.
24. Yunoki S, Ikoma T, Tsuchiya A, Monkawa A, Ohta K, Sotome S, Shinomiya K, Tanaka J. Fabrication and mechanical and tissue ingrowth properties of unidirectionally porous hydroxyapatite/collagen composite. J Biomed Mater Res B: Appl Biomater 2007;80:166–173.
25. Kim HW, Knowles JC, Kim HE. Hydroxyapatite porous scaffold engineered with biological polymer hybrid coating for antibiotic vancomycin release. J Mater Sci Mater Med 2005; 16:189–195.
26. Callcut S, Knowles JC. Correlation between structure and compressive strength in a reticulate glass-reinforced hydroxyapatite foam. J Mater Sci: Mater Med 2002;13:485–489.
27. Ramay HRR, Zhang M. Preparation of porous hydroxyapatite scaffolds by combination of the gel-casting and polymer sponge methods. Biomaterials 2003;24:3293–3302.
28. Chen QZ, Thompson ID, Boccaccini AR. 45S5 Bioglass®-derived glass-ceramic scaffold for bone tissue engineering. Biomaterials 2006;27:2414–2425.
29. Wu C, Chang J, Zhai W, Ni S, Wang J. Porous akermanite scaffolds for bone tissue engineering: Preparation, characterization, and in vitro studies. J Biomed Mater Res B: Appl Biomater 2006;78:47–55.
30. Sepulveda P, Ortega FS, Innocentini MDM, Pandolfelli VC. Properties of highly porous hydroxyapatite obtained by the gelcasting of foams. J Am Ceram Soc 2000;83:3021–3024.
31. Fu Q, Rahaman MN, Bal BS, Huang W, Day DE Preparation and bioactive characterization of a porous 13-93 glass, and fabrication into the articulating surface of a proximal tibia. J Biomed Mater Res A 2007;82:222–229.
32. Cyster LA, Grang DM, Howdle SM, Rose FRAJ, Irvine DJ, Freeman D, Scotchfor CA, Shakesheff KM. The influence of dispersant concentration on the pore morphology of hydroxyapatite ceramics for bone tissue engineering. Biomaterials 2005;26:697–702.
33. Harris LD, Kim BS, Mooney DJ. Open pore biodegradable matrices formed with gas foaming. J Biomed Mater Res 1998;42:396–402.
34. Chang BS, Lee CK, Hong KS, Youn HJ, Syu HS, Chung SS, Park KW. Osteoconduction at porous hydroxyapatite with various pore configurations. Biomaterials 2000;21:1291–1298.
35. Schoof H, Apel J, Heschel I, Rau G. Control of pore structure and size in freeze-dried collagen sponges. J Biomed Mater Res Appl Biomater 2001;58:352–357.
36. Rahaman MN. Ceramic Processing and Sintering, 2nd ed. New York: Marcel Dekker; 2003. pp 591–592.
37. Chaki TK, Wang PE. Densification and strengthening of silver-reinforced hydroxyapatite-matrix composite prepared by sintering. J Mater Sci Mater Med 1994;5:533–542.
38. Ruys AJ, Wei M, Sorrell CC, Dickson MR, Brandwood A, Milthorpe BK. Sintering effects on the strength of hydroxyapatite. Biomaterials 1995;16:409–415.
39. Yamada S, Heymann D, Bouler JM, Daculsi G. Osteoclastic resorption of calcium phosphate ceramics with different hydroxyapatite/tricalcium phosphate ratios. Biomaterials 1997; 18:1037–1041.
40. Hulbert SF, Young FA, Mathews RS, Klawitter JJ, Talbert CD, Stelling FH. Potential of ceramic materials as permanently implantable skeletal prostheses. J Biomed Mater Res 1970;4:433–456.
41. Hollinger JO, Brekke J, Gruskin E, Lee D. Role of bone substitutes. Clin Orthop Relat Res 1996;324:55–65.
42. Sarikaya M. An introduction to biomimetics: A structural viewpoint. Microsc Res Tech 1994;27:360–375.
43. Carter DR. Bone compressive strength: The influence of density and strain rate. Science 1976;194:1174–1176.
44. Linde F, Norgaard P, Hvid I, Odgaard A, Soballe KM. Mechanical properties of trabecular bone. Dependency on strain rate. J Biomech 1991;24:803–809.
45. Wachtman JB. Mechanical Properties of Ceramics. New York: Wiley; 1996. pp 159–163.
46. Gibson LJ, Ashby MF. Cellular Solids: Structure and Properties. New York: Cambridge University Press; 1997.